ChemComm

COMMUNICATION

View Article Online
View Journal

Cite this: DOI: 10.1039/d5cc07117h

Received 15th December 2025,
Accepted 29th April 2026

DOI: 10.1039/d5cc07117h

rsc.li/chemcomm

Active-template CuAAC enables high-yield synthesis of (2)handcuff [2]rotaxanes

Arjun Veliyil Prakash, Helal Metawi and Abed Saady *

An active-template CuAAC strategy enables the efficient synthesis of (2)handcuff [2]rotaxanes in high isolated yields. A bis-2,2′-bipyridine macrocycle acts as a Cu^{I} ligand that templates dual CuAAC reactions and enforces the dual-threaded handcuff architecture. This approach provides a concise and practical route to higher-order mechanically interlocked architectures.

Mechanically interlocked molecules (MIMs),[1] including catenanes, rotaxanes, and their higher-order analogues, provide synthetically accessible entry points for controlled molecular motion,[2–4] topological chirality,[5–7] and programmable supramolecular behaviour.[8–11] The continuing expansion of this field has enabled sophisticated molecular machines,[12] redox-active assemblies,[13] and switchable host–guest systems,[14] whose properties arise directly from the constraints imposed by the mechanical bond. As highlighted by Beer, Sauvage, Stoddart, and others, the fundamental challenge remains the efficient, predictable synthesis of increasingly complex interlocked architectures.[15–19] Among these, handcuff architectures, in which two covalently linked macrocycles cooperatively bind and mechanically interlock one or more threads, occupy a special position due to their structural rigidity and emergent functional behaviour.[20–23]

Early examples of handcuff assemblies were accessed using cation or anion templation and π-donor/acceptor interactions, demonstrating how cooperative noncovalent interactions can stabilise higher-order interlocked architectures and enable functional behaviour.[24–30] More recently, bis-macrocyclic hosts have been used to engineer rigid molecular handcuffs capable of positioning redox-active chromophores to enable excimer emission, radical-ion π-dimers, or controlled electron transfer between co-facially arranged dyes.[31] These systems underscore the extraordinary potential of the handcuff motif for organising functional units while still permitting dynamic response.

Despite these advances, synthetic access to handcuff rotaxanes remains limited. Most strategies employ either passive templation and stoppering of a single axle threading both rings, often with demanding macrocycle syntheses, or covalent linking of axles that pass individually through each macrocycle, a strategy that has only rarely been demonstrated. Recently, Evans and co-workers showed that copper-catalysed azide–alkyne cycloaddition (CuAAC) can link two independently threaded axles inside a bis-macrocycle, but yields remain modest, highlighting the need for further optimisation of the methodology.[32] Likewise, the broader review by Champness and co-workers emphasises that handcuff rotaxanes constitute one of the least explored classes of MIMs, in part due to the lack of efficient synthetic tools capable of reliably constructing them.[21]

In parallel, active-template (AT) reactions, pioneered by Leigh and further developed by Goldup and others, have transformed the synthesis of MIMs by allowing the metal catalyst not only to mediate covalent bond formation but also to template the assembly of the mechanical bond. Among these, the AT-CuAAC reaction is particularly powerful due to its mild conditions, functional group tolerance, and ability to operate in sterically demanding environments that arise during mechanical bond formation.[33–40]

Here, we merge the structural advantages of 2,2′-bipyridine-based bis-macrocycles with the synthetic power of AT-CuAAC to develop a practical, concise, and high-yielding route to (2)handcuff [2]rotaxanes. In our design, the bis-2,2′-bipyridine acts as a ligand for Cu^{I}, providing two potential metal-binding sites and serving as a template for mechanical bond formation. This strategy overcomes key limitations of earlier approaches, namely low yields and long synthetic sequences, providing a modular, programmable platform for constructing (2)handcuff [2]rotaxanes under mild conditions.

The resulting interlocked molecules expand the accessible chemical space of higher-order MIM architectures and provide a foundation for future studies on motion, redox activity, and potential nanotechnology applications in multicomponent mechanically interlocked systems.

Our study began with the design of a synthetically accessible, symmetrically substituted 2,2′-bipyridine macro-cycle that

Department of Chemistry, Bar-Ilan University, Ramat-Gan, 52900, Israel.
E-mail: Abed.saady@biu.ac.il

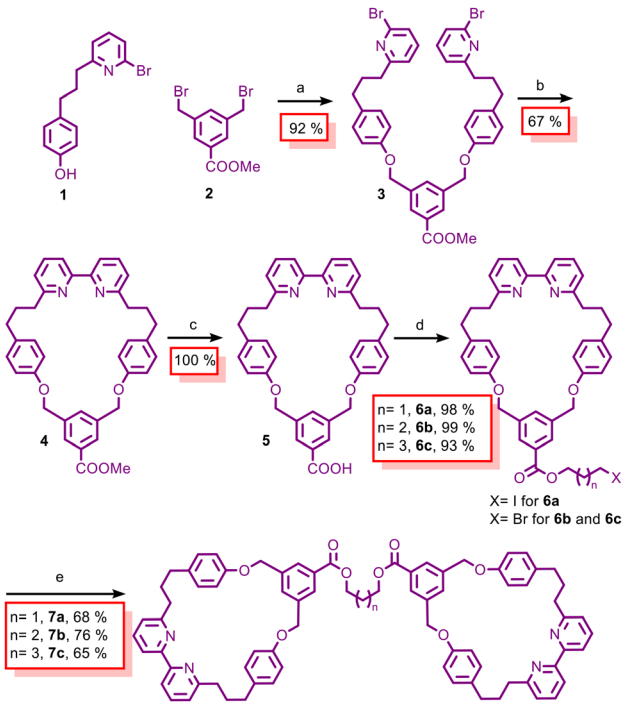

Scheme 1 Synthesis of bis-2,2′-bipyridine macrocycles **7a–c**. Reagents and conditions: (a) K_2CO_3, MeCN, reflux, 12 h, 92% yield. (b) $Ni(PPh_3)_2Br_2$, NEt_4I, PPh_3, Mn, DMF, 50 °C, 4 h, 67% yield. (c) NaOH, THF : H_2O, r.t., 100% yield. (d) 1,3-Diiodopropane for **6a**, 1,4-dibromobutane for **6b** and 1,5-dibromopentane for **6c**, K_2CO_3, MeCN, 50 °C, 12 h, 93–99% yield. (e) **5**, K_2CO_3, MeCN, 50 °C, 12 h, 65–76% yield.

could be readily diversified and dimerized to form a bis-2,2′-bipyridine macrocycle scaffold specifically tailored for AT-CuAAC assembly of handcuff rotaxanes while avoiding the formation of mechanically chiral isomers.[41–43] A key feature of this design is the incorporation of an ester linkage that provides a convenient and high-yielding route to the bis-2,2′-bipyridine macrocycles used in the AT-CuAAC assembly.

Bis-2,2′-bipyridine macrocycles **7a–c** were prepared *via* a concise multi-step sequence involving Ni-mediated macrocyclisation[44] and subsequent functionalisation (Scheme 1; see the SI for full details).[45]

To access the targeted (2)handcuff [2]rotaxanes **10a–c**, we first prepared 1-azido-3,5-di-*tert*-butylbenzene (**8**) and *N*1,*N*3-di(prop-2-yn-1-yl)isophthalamide (**9**) according to previously reported procedures.[44,46] Azide **8** was selected as a commonly used bulky stopper suitable for macrocycles of this size, whereas bis-alkyne **9** served as a stable axle bearing two alkyne units that enabled dual AT-CuAAC bond formation within the bis-macrocyclic scaffold.

Scheme 2 illustrates the AT-CuAAC assembly of (2)handcuff [2]rotaxanes **10a–c** from bis-macrocycles **7a–c**, bis-alkyne **9**, and azide **8**. The bis-macrocyclic bipyridine framework defines two Cu^I-binding cavities that enable sequential active-template CuAAC bond-forming events leading to the dual-threaded handcuff architecture. The AT-CuAAC reactions were conducted using equimolar amounts of bis-macrocycle and bis-alkyne, together with two equivalents of azide **8** and

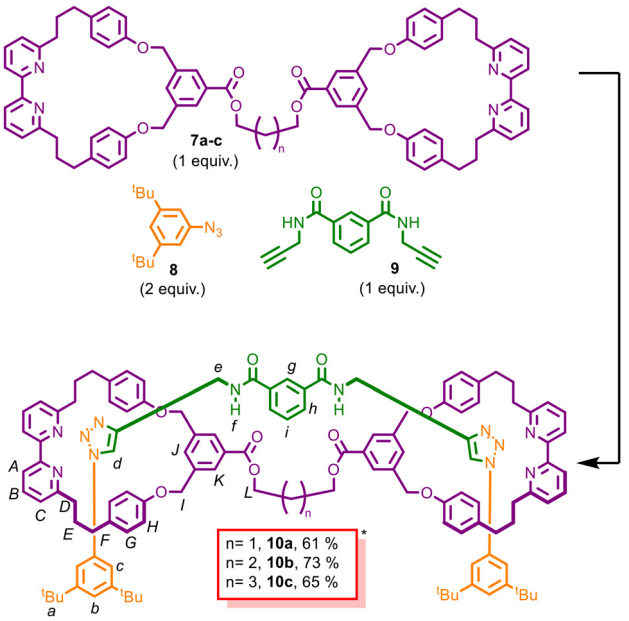

Scheme 2 Synthesis of (2)handcuff [2]rotaxanes **10a–c**. Reagents and conditions: $[Cu(CH_3CN)]PF_6$ (2 equiv.), $^iPr_2NEt$ (4 equiv.), CH_2Cl_2, 16 h, 61–73% yield. *The yields are calculated based on the average of two reactions. Reactions were conducted at 0.005 M with respect to the bis-macrocycle; the effect of concentration on product formation was examined and is discussed in the SI.

$[Cu(CH_3CN)]PF_6$, matching the two required CuAAC bond-forming events.

Under these conditions, treatment of bis-macrocycles **7a–c** with bis-alkyne **9**, azide **8**, and the Cu(I) catalyst afforded the corresponding (2)handcuff [2]rotaxanes **10a–c** in high isolated yields. The reaction is consistent with a pathway in which sequential AT-CuAAC bond formation within the bis-macrocyclic scaffold leads to selective handcuff assembly.

Pleasingly, our first active-template experiment employing bis-macrocycle **7a** delivered the desired (2)handcuff [2]rotaxane in 61% isolated yield, demonstrating the efficiency of the AT-CuAAC strategy for assembling this higher-order interlocked structure. Evidence for successful rotaxane formation was provided by high-resolution mass spectrometry (HRMS; observed *m*/*z* for $[C_{119}H_{126}N_{12}O_{10}]^+$ = 1884.9816, calculated 1884.9811; Fig. S61) and by comprehensive NMR analysis. 1D and key 2D NMR experiments (COSY, HMQC, and HMBC) were acquired for all compounds, enabling further signal assignments and supporting the proposed interlocked architectures (see the SI).

The ^1H NMR spectra of (2)handcuff [2]rotaxane **10a**, along with those of bis-macrocycle **7a** and non-interlocked axle **S1** for comparison, are shown in Fig. 1.[47] Comparison of the ^1H NMR spectra of (2)handcuff [2]rotaxane **10a** with those of the parent bis-macrocycle **7a** and the independently synthesized axle **S1** reveals pronounced and diagnostic changes that unequivocally confirm mechanical bond formation. In contrast to many AT-CuAAC rotaxanes, where the most dramatic perturbations are typically observed for the triazole C–H proton,[34] the major chemical shift changes in our system occur on the axle protons rather than at the triazole C–H site.

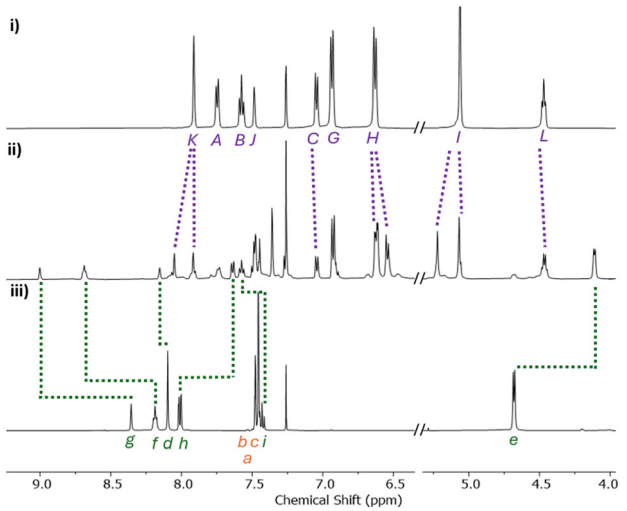

Fig. 1 Partial ^{1}H NMR ($CDCl_3$, 500 MHz, 298 K) spectra of (i) bis-macrocycle **7a**, (ii) (2)handcuff [2]rotaxane **10a**, and (iii) axle **S1**.

The amide-adjacent resonances H_h ($\Delta\delta \approx 0.64$ ppm) and H_g ($\Delta\delta \approx 0.1$ ppm) exhibit substantial downfield shifts relative to **S1**, indicating a markedly different chemical environment for the threaded axle in the interlocked structure. Proton H_d (triazole C–H), which often serves as a key diagnostic resonance in CuAAC-derived rotaxanes, displays only a modest change in chemical shift relative to **S1**. Together, these data suggest that the bis-macrocycle resides preferentially over the amide-containing region of the axle rather than over the triazole unit.

In addition to these axle-centered perturbations, several macrocycle protons undergo characteristic mechanical bond induced changes. Protons H_L, H_I, H_H, and H_K convert from singlets in the free bis-macrocycle to well-resolved geminal doublets in the (2)handcuff [2]rotaxane, reflecting facial desymmetrisation of the bipyridine scaffold when the axle is threaded through the dual cavities. These observations are consistent with similar behaviour reported recently for related pyridine-based interlocked systems.[32] Notably, the axle proton H_e is shifted upfield ($\Delta\delta \approx 0.6$ ppm). This pronounced shielding effect arises because, in the (2)handcuff [2]rotaxane architecture, the proton sits in a more crowded and enclosed environment than in the free axle. When protons are positioned close to aromatic rings, they often experience a local magnetic environment that reduces their chemical shift. In this case, the proximity of proton H_e to the bipyridine rings and to the folded conformation enforced by the mechanical bond places it in a region where the aromatic system partially shields it from the external magnetic field. As a result, an upfield shift is observed. Such through-space shielding effects are familiar features of interlocked molecules and other systems in which aromatic rings and nearby protons adopt well-defined spatial relationships.

Taken together, these observations provide a clear spectroscopic fingerprint for the dual-threaded architecture. Importantly, the same qualitative NMR features were observed for (2)handcuff [2]rotaxanes **10b** and **10c**, demonstrating that the mechanical environment is preserved across the bis-macrocycles. Notably, varying the length of the alkyl linker in bis-macrocycles **7a–c** had little influence on the efficiency of the AT-CuAAC process, with all three scaffolds delivering the corresponding (2)handcuff [2]rotaxanes in similarly high yields.[48] The small variations in isolated yield across **10a–c** fall within the expected experimental range and did not correlate with linker length. To the best of our knowledge, these are among the highest isolated yields reported for (2)handcuff [2]rotaxane synthesis.

Notably, the reaction of bis-macrocycle **7b**, bis-alkyne **9**, and azide **8** under otherwise analogous conditions in CH_2Cl_2/MeOH (1 : 1) gave a markedly different outcome, with only a low isolated yield of the target (2)handcuff [2]rotaxane and a more complex crude reaction profile (see the SI for details). This result highlights the strong sensitivity of the assembly process to solvent environment; however, the origin of this effect cannot be assigned unambiguously based on the present data.

In summary, we have developed an active-template CuAAC strategy for the efficient construction of (2)handcuff [2]rotaxanes using bis-2,2′-bipyridine macrocycles. Sequential active-template CuAAC bond formation within the bis-macrocyclic scaffold delivers the interlocked products in high isolated yields, among the highest reported for (2)handcuff [2]rotaxane synthesis. The robustness of this approach across a small macrocycle series highlights its utility as a practical route to higher-order mechanically interlocked architectures. This platform is now being extended to handcuff catenanes and additional functional architectures, and these results will be reported in due course.

Conflicts of interest

There are no conflicts to declare.

Data availability

The data supporting this article have been included as part of the supplementary information (SI). Supplementary information: procedures and characterization data (NMR and MS) for all new compounds. See DOI: https://doi.org/10.1039/d5cc07117h.

Acknowledgements

Abed Saady thanks Bar-Ilan University (start-up grant) and the Council for Higher Education (MAOF scholarship). The authors thank Dr Yulia Shenberger (BIU) for recording the HRMS spectra for all the reported compounds.

References

1 J. F. Stoddart, *Angew. Chem., Int. Ed.*, 2017, **56**, 11094.
2 J. J. Davis, G. A. Orlowski, H. Rahman and P. D. Beer, *Chem. Commun.*, 2010, **46**, 54–63.
3 C. J. Bruns and J. F. Stoddart, *Acc. Chem. Res.*, 2014, **47**, 2186–2199.
4 J.-P. Sauvage, *Acc. Chem. Res.*, 1998, **31**, 611–619.
5 E. Jamieson, F. Modicom and S. Goldup, *Chem. Soc. Rev.*, 2018, **47**, 5266–5311.
6 J. E. Lewis, M. Galli and S. M. Goldup, *Chem. Commun.*, 2017, **53**, 298–312.
7 N. H. Evans, *Chem. – Eur. J.*, 2018, **24**, 3101–3112.

8 G. Washino, M. A. Soto, S. Wolff and M. J. MacLachlan, *Commun. Chem.*, 2022, **5**, 155.
9 A. Saady, G. K. Malcolm, M. P. Fitzpatrick, N. Pairault, G. J. Tizzard, S. Mohammed, A. Tavassoli and S. M. Goldup, *Angew. Chem., Int. Ed.*, 2024, **63**, e202400344.
10 S. Paryente, H. Aledwan and A. Saady, *Commun. Chem.*, 2025, **8**, 149.
11 R. Barat, T. Legigan, I. Tranoy-Opalinski, B. Renoux, E. Péraudeau, J. Clarhaut, P. Poinot, A. E. Fernandes, V. Aucagne and D. A. Leigh, *Chem. Sci.*, 2015, **6**, 2608–2613.
12 Y. Feng, M. Ovalle, J. S. Seale, C. K. Lee, D. J. Kim, R. D. Astumian and J. F. Stoddart, *J. Am. Chem. Soc.*, 2021, **143**, 5569–5591.
13 M. Baroncini, S. Silvi and A. Credi, *Chem. Rev.*, 2019, **120**, 200–268.
14 M. N. Chatterjee, E. R. Kay and D. A. Leigh, *J. Am. Chem. Soc.*, 2006, **128**, 4058–4073.
15 J. P. Sauvage, *Angew. Chem., Int. Ed.*, 2017, **56**, 11080–11093.
16 J. E. Lewis, P. D. Beer, S. J. Loeb and S. M. Goldup, *Chem. Soc. Rev.*, 2017, **46**, 2577–2591.
17 X. Hou, C. Ke and J. F. Stoddart, *Chem. Soc. Rev.*, 2016, **45**, 3766–3780.
18 A. Saady and S. M. Goldup, *Chemistry*, 2023, **9**, 2110–2127.
19 N. H. Evans, *Eur. J. Org. Chem.*, 2019, 3320–3343.
20 N. H. Evans, C. J. Serpell and P. D. Beer, *Angew. Chem., Int. Ed.*, 2011, **50**, 2507–2510.
21 N. Pearce, M. Tarnowska, N. J. Andersen, A. Wahrhaftig-Lewis, B. S. Pilgrim and N. R. Champness, *Chem. Sci.*, 2022, **13**, 3915–3941.
22 S. Tajima, A. Muranaka, M. Naito, N. Taniguch, M. Harada, S. Miyagawa, M. Ueda, H. Takaya, N. Kobayashi and M. Uchiyama, *Org. Lett.*, 2021, **23**, 8678–8682.
23 T. Tsukamoto, R. Sasahara, A. Muranaka, Y. Miura, Y. Suzuki, M. Kimura, S. Miyagawa, T. Kawasaki, N. Kobayashi and M. Uchiyama, *Org. Lett.*, 2018, **20**, 4745–4748.
24 K. J. Hartlieb, A. K. Blackburn, S. T. Schneebeli, R. S. Forgan, A. A. Sarjeant, C. L. Stern, D. Cao and J. F. Stoddart, *Chem. Sci.*, 2014, **5**, 90–100.
25 R. Ciao, C. Talotta, C. Gaeta, L. Margarucci, A. Casapullo and P. Neri, *Org. Lett.*, 2013, **15**, 5694–5697.
26 H. Iwamoto, Y. Yawata, Y. Fukazawa and T. Haino, *Chem. Lett.*, 2010, **39**, 24–25.
27 Z.-J. Zhang, M. Han, H.-Y. Zhang and Y. Liu, *Org. Lett.*, 2013, **15**, 1698–1701.
28 Y.-X. Ma, Z. Meng and C.-F. Chen, *Org. Lett.*, 2014, **16**, 1860–1863.
29 H. V. Schröder, H. Hupatz, A. J. Achazi, S. Sobottka, B. Sarkar, B. Paulus and C. A. Schalley, *Chem. – Eur. J.*, 2017, **23**, 2960–2967.
30 T. Sato and T. Takata, *Tetrahedron Lett.*, 2007, **48**, 2797–2801.
31 L. Yang, P. Langer, E. S. Davies, M. Baldoni, K. Wickham, N. A. Besley, E. Besley and N. R. Champness, *Chem. Sci.*, 2019, **10**, 3723–3732.
32 S. R. Barlow, D. Tomkinson, N. R. Halcovitch and N. H. Evans, *Org. Biomol. Chem.*, 2024, **22**, 5393–5400.
33 V. Aucagne, K. D. Hänni, D. A. Leigh, P. J. Lusby and D. B. Walker, *J. Am. Chem. Soc.*, 2006, **128**, 2186–2187.
34 H. Lahlali, K. Jobe, M. Watkinson and S. M. Goldup, *Angew. Chem., Int. Ed.*, 2011, **50**, 4151–4155.
35 R. Jamagne, M. J. Power, Z.-H. Zhang, G. Zango, B. Gibber and D. A. Leigh, *Chem. Soc. Rev.*, 2024, **53**, 10216–10252.
36 S. Saito, E. Takahashi and K. Nakazono, *Org. Lett.*, 2006, **8**, 5133–5136.
37 Y. Sato, R. Yamasaki and S. Saito, *Angew. Chem., Int. Ed.*, 2009, **48**, 504–507.
38 J. M. Van Raden, N. N. Jarenwattananon, L. N. Zakharov and R. Jasti, *Chem. – Eur. J.*, 2020, **26**, 10205–10209.
39 J. H. May, J. M. Fehr, J. C. Lorenz, L. N. Zakharov and R. Jasti, *Angew. Chem., Int. Ed.*, 2024, **136**, e202401823.
40 J. H. May, J. M. Van Raden, R. L. Maust, L. N. Zakharov and R. Jasti, *Nat. Chem.*, 2023, **15**, 170–176.
41 A. Savoini, P. R. Gallagher, A. Saady and S. M. Goldup, *J. Am. Chem. Soc.*, 2024, **146**, 8472–8479.
42 P. R. Gallagher, A. Savoini, A. Saady, J. R. Maynard, P. W. Butler, G. J. Tizzard and S. M. Goldup, *J. Am. Chem. Soc.*, 2024, **146**, 9134–9141.
43 S. Zhang, A. Rodríguez-Rubio, A. Saady, G. J. Tizzard and S. M. Goldup, *Chemistry*, 2023, **9**, 1195–1207.
44 J. Lewis, R. Bordoli, M. Denis, C. Fletcher, M. Galli, E. Neal, E. Rochette and S. Goldup, *Chem. Sci.*, 2016, **7**, 3154–3161.
45 A stepwise linking strategy was employed to ensure clean and reproducible formation of bis-macrocycles **7a–c**, as one-step approaches led to complex mixtures and reduced efficiency.
46 Y. Xu, M. D. Smith, M. F. Geer, P. J. Pellechia, J. C. Brown, A. C. Wibowo and L. S. Shimizu, *J. Am. Chem. Soc.*, 2010, **132**, 5334–5335.
47 Minor additional signals are observed in the ^{1}H NMR spectra of compounds **10a–c**. On the basis of LC–MS analysis, which shows a single dominant chromatographic peak corresponding to the expected molecular ion, these signals are most likely attributed to amide rotamers within the interlocked framework.
48 The crude reaction mixtures were analysed by mass spectrometry prior to purification; see the SI for details.

